energies

MDPI

Article

Improving the Penetration of Wind Power with Dynamic Thermal Rating System, Static VAR Compensator and Multi-Objective Genetic Algorithm

Jiashen Teh [1,*], Ching-Ming Lai [2] and Yu-Huei Cheng [3]

1 School of Electrical and Electronic Engineering, Universiti Sains Malaysia (USM), 14300 Nibong Tebal, Penang, Malaysia
2 Department of Vehicle Engineering, National Taipei University of Technology, 1, Sec. 3, Chung-Hsiao E. Road, Taipei 10608, Taiwan; pecmlai@gmail.com
3 Department of Information and Communication Engineering, Chaoyang University of Technology, Taichung 41349, Taiwan; yuhuei.cheng@gmail.com
* Correspondence: jiashenteh@usm.my; Tel.: +60-04-599-6016

Received: 5 March 2018; Accepted: 27 March 2018; Published: 2 April 2018

Abstract: The integration of renewable energy sources, especially wind energy, has been on the rise throughout power systems worldwide. Due to this relatively new introduction, the integration of wind energy is often not optimized. Moreover, owing to the technical constraints and transmission congestions of the power network, most of the wind energy has to be curtailed. Due to various factors that influence the connectivity of wind energy, this paper proposes a well-organized posterior multi-objective (MO) optimization algorithm for maximizing the connections of wind energy. In this regard, the dynamic thermal rating (DTR) system and the static VAR compensator (SVC) have been identified as effective tools for improving the loadability of the network. The propose MO algorithm in this paper aims to minimize: (1) wind energy curtailment, (2) operation cost of the network considering all investments and operations, also known as the total social cost, and (3) SVC operation cost. The proposed MO problem was solved using the non-dominated sorting genetic algorithm (NSGA) II and it was tested on the modified IEEE reliability test system (IEEE-RTS). The results demonstrate the applicability of the proposed algorithm in aiding power system enhancement planning for integrating wind energy.

Keywords: wind energy; dynamic thermal rating system; reliability; renewable energy; genetic algorithm

1. Introduction

In the midst of uncertain fossil fuel price due to constant geopolitical shifts and its harmful effects on climate change, wind power has emerged as a global promising alternative source for electric power generation. Due to this, wind energy has experienced fast growth over the last decades. For example, in 2016 alone, more than 54 GW of wind power was installed globally in more than 90 countries, marking a 12.6% growth of wind capacity worldwide and this addition raises the global cumulative wind capacity to 486.8 GW [1]. Much of this growth is motivated by various incentive programs and binding regulations, which are all designed to increase the wind power quota within existing generation portfolios of the power systems. According to the Energy Roadmap 2050 of the European Commission, the greenhouse gas emission will be reduced by 80–95% in order to achieve a low-carbon economy across Europe by 2050 [2]. This, however, can only be achieved if 97% of the power supply in Europe is derived from renewable energy sources [3]. In a similar effort, the Australian government aim to have one third of their electricity generated by renewable sources by 2020.

The inherent volatility of wind speed causes the generation of wind power to be non-dispatchable and uncertain. Hence, unlike the conventional generation units powered by fossil fuel, wind as an intermittent energy source cannot provide "firm" power connection. In certain conditions that violate power system security constraints and operating limits, a portion of the available wind power has to be curtailed [4]. This presents a non-desirable condition as the system operator, under the contractual obligations with wind farm generators, has to keep the wind curtailment below a prescribed level [5]. Among the reasons for wind energy curtailment, transmission network congestions and the temporal mismatch between load and available wind power top the list. The issue of wind curtailment is further aggravated by the fact that thermal generators cannot operate at a very low level due to the minimum generation requirement for maintaining dynamic stability of the power systems [6]. These interactions complicate the operations of wind farms and remedial actions have to be taken if high wind integration in the power systems is to be achieved.

A simple solution to the above problem is to undertake the transmission expansion planning (TEP) project to reduce line congestions and increase transmission capacity to integrate more wind power [7,8]. The studies on TEP for the purpose of aiding wind power integrations are well covered in the literature. A study on the TEP model for integrating the large amount of remote wind power was investigated and proven beneficial [8]. A probabilistic TEP strategy was proposed in a two-part paper [9,10]. In it, the random nature of wind was modelled, but the effects of wind energy curtailment were not considered in the planning that have only risk and investment costs. A probabilistic TEP approach that considered load and wind power generation uncertainties was proposed [11]. This paper utilized the Benders decomposition algorithm in conjunction with the Monte Carlo simulation to tackle the proposed probabilistic TEP. Finally, a study has also investigated the capacity expansion planning that would be required to integrate future wind generation surplus [12]. Nonetheless, TEP projects normally have long lead time and are very expensive. The expansion of the transmission network may also be inhibited due to space limitations and state regulations for environmental conservation [13]. Economically, transmission network expansions for the sake of reducing wind curtailment may also not be the most optimum investment decision [14].

Hence, an alternative to the TEP is to use the state-of-the-art dynamic thermal rating (DTR) system that is able to increase the capacity of existing transmission lines based on various weather conditions, especially wind. Various studies that have highlighted the advantages of the DTR system in aiding the integration of wind power are given next. A methodology that optimally deploys DTR sensors on the identified critical spans of the lines was proposed and it was deduced that this has the potential to maximize wind integrations [15]. From a system-wide perspective, the DTR system was demonstrated as an efficient tool in integrating the large amount of wind power [16]. The DTR system was also shown to be able to estimate the line rating potential and the additional wind energy that can be accommodated on a DTR-enhanced line [17]. Finally, the DTR system is also able to coordinate with demand response technology for increasing the utilization of wind generation [18]. Apart from the DTR system, the flexible AC transmission system (FACTS) device is another technology beneficial for wind integration by improving the conditions of the network. These conditions are identified as minimum power losses, improved voltage profiles and maximum system loadability [19–21]. The interactions between FACTS and renewable sources have been investigated in a number of studies [22–24]. In these studies, optimal criterion such as location and size of the devices were considered. They, however, assume only an intact system for the studies.

The aforementioned studies dealt with the application of technologies for improving wind energy usage. From the perspective of improving power system operation, an evaluation on the impact of wind energy towards the reliability of a small isolated power system was presented [25]. Stochastic unit commitment with wind generation was studied so that greater wind power penetration can be achieved without sacrificing security [26]. Using a novel linear programming optimization model, the maximum wind energy connection for a given network was estimated [27]. In this study, the usage of a probabilistic approach in order to satisfy the contracted wind energy on an annual basis was neglected. In cases where the probabilistic wind modelling was used, wind curtailment and its joint consideration with load were not accounted for [7,28,29].

All the literature surveyed above demonstrated that while there are many individual works that look into the usage of the DTR system, FACTS devices, and advance power system management methods for the optimal integration of wind energy, there is still a need for a similar but comprehensive study that combines all three elements. Owing to this gap, this paper investigates the usage of the DTR system and FACTS device as a long-term solution for curbing wind energy curtailment in the power systems. This is achieved through a novel planning methodology that employs the multi-objective (MO) variant of the genetic optimization algorithm. The proposed approach considers wind energy curtailment cost, total social cost and FACTS device operational cost. To the author's best knowledge, it is for the first time that such an integrated planning effort is carried out. The proposed method was tested on the IEEE 24-bus reliability test system (IEEE-RTS) [30] and the results are thoroughly analyzed in this paper.

2. Problem Description

The abilities of FACTS devices in controlling the AC transmission system parameters and providing reactive power compensation are an unavoidable complement to the addition of wind farms. Reactive power compensation is needed as the delivery system (transmission line) and loads consume reactive power, the flow of reactive power from sources to sinks causes line heating and voltage drop in the network, and the generation of reactive power can limit the generation of real power. In this paper, the static VAR compensator (SVC), a parallel connected FACTS device, is utilized as the reactive compensator. The SVC controls the nodal voltage through injection and absorption of reactive power.

Figure 1a shows a simple power system divided into two areas: west and east. Assume that the west area has a total wind farm capacity of 9000 MW with a sufficiently large reactive source of 3500 MVR, whereas the east area consists of the conventional 3000 MW thermal generators and a limited reactive capacity of 500 MVR. The loads in both areas are consuming 6000 MW and 1000 MVR each. The line capacity in between these areas is assumed to be 2000 MW after being enhanced by the DTR system. Despite the enhancement, the line load flow is limited to only 1000 MW as shown in Figure 1a and this causes a load curtailment of 2000 MW in the east area. The reason for the underutilization of the line is a high capacity line will not carry its share of line loading based only on its high capacity margin alone. The load flow is also governed by its impedance and other AC transmission system parameters. In contrast, when the SVC with a reactive capacity of 500 MVR is installed in the east area as shown in Figure 1b, the line load flow is raised by 800 MW and consequently reducing the load curtailment by the same amount. This also shows that the SVC enables higher amount of wind energy integration and reduces the wind energy curtailment by 800 MW. Hence, a comprehensive cost/benefit analysis of SVC is required to determine the ability of the technology in aiding the integration of wind energy. Such a study will help power system operator in optimistically looking forward to a higher amount of wind energy connection in order to serve more electrical loads.

Based on the above discussion, a comprehensive study that is aimed at reducing the wind energy curtailment by optimizing the location of SVC along with the strategic transmission line enhancement by the DTR system is needed. Although the implementation of this study will increase the power system investment cost, it will generally improve the integration of wind energy, relieve transmission line congestion during on-peak times, and reduce the dependency on conventional thermal generators. It is noted that although the wind energy curtailment cost might be lower than the additional costs due to the investments and operations of the new technologies, this cost will be greatly aggravated in a highly wind penetrated scenario. Moreover, various renewable energy policies implemented around the world that penalize wind energy curtailment forces system operators to more cautiously face the issue. Hence, the costs and benefits of the SVC and DTR system need to be properly modelled in the planning studies for optimizing the operation of the power system in order to minimize wind energy curtailment.

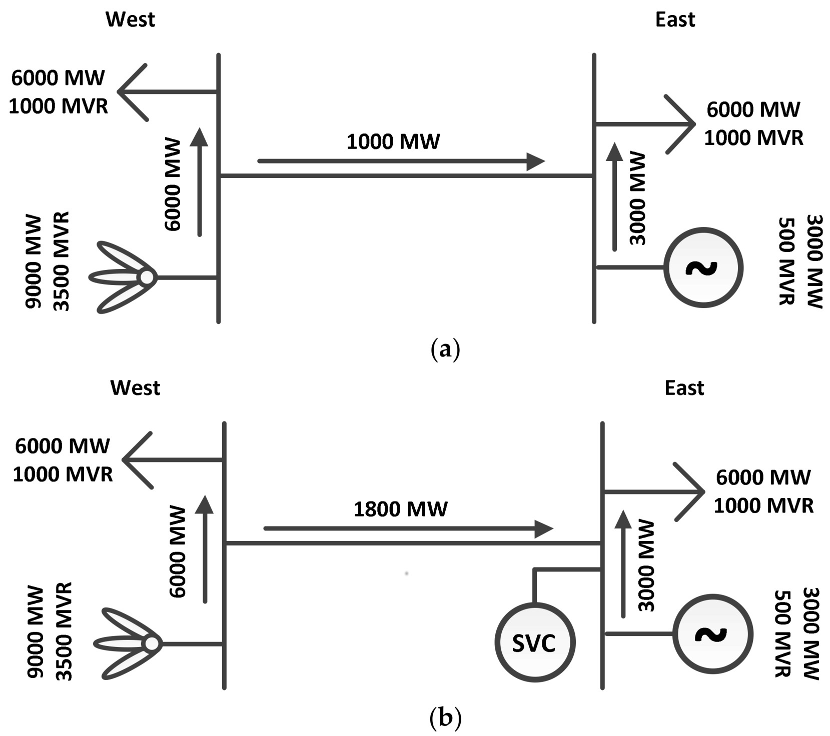

Figure 1. Power system: (**a**) without static VAR compensator (SVC) and (**b**) with SVC.

Considering that the wind energy curtailment cost, thermal generator fossil fuel cost, the SVC and DTR system costs cannot be considered in the same way, a posterior optimization approach is instead presented in this paper to determine the optimal combinations of the SVCs and DTR systems in order to minimize wind energy curtailment. The main feature of the proposed optimization is that different costs are separately considered rather than as a whole. As a result, this becomes a multi-objectives (MO) optimization problem whereby some optimal plans are found. In this paper, the following objective functions (costs) are considered:

- Wind energy curtailment cost
  A penalty cost is attached to every unit of wind energy curtailment. By doing this, wind energy curtailment is minimized by reducing the wind energy curtailment cost.
- Social cost
  This consists of the investment costs of the SVCs and DTR systems, transmission line congestion cost, load curtailment cost, and the fossil fuel cost of the thermal generators.
- SVC operational cost
  An operation cost is attached to every unit of reactive power produced by the SVC. Minimizing this cost is equivalent to minimizing the production of the reactive power.

The above costs are considered conflicting as no cost terms can be reduced without increasing the other costs. For example, the wind energy curtailment cost can be reduced only by installing more DTR systems and SVCs. This, however, is an additional investment into the network and is sometimes not possible due to budget limitations. An equally applicable example is the system operator might want to limit the usage of the SVC to lower the operation cost but this has the consequence of higher wind energy curtailment. Then, the attempt to lower wind energy curtailment will necessarily increase the operation of the SVC and subsequently the operation cost. Therefore, the three cost terms presented above cannot be viewed as the same and should be considered as conflicting objectives instead.

3. Methodology

3.1. Wind Farm Model

The modelling of wind farm consist of two parts: the natural wind speed and the wind turbine curve that translates wind speed into wind power. The wind speed, contrary to the main assumption of it being entirely random, actually propagates through time in a manner that exhibits trends affected by its past behavior [31]. An appropriate way to model this kind of data is to use the auto-regression moving-average (ARMA) model [16,31]. Through the ARMA model, the time-series wind speed can be simulated by following its actual propagation trend. Then, the wind power outputs are produced according to its non-linear relationship (wind power curve) with the wind speeds [31]. Through these, both the wind speeds and the wind power outputs are expressed in a chronological manner. In this paper, the wind power curve from the Vestas V90 three-megawatt wind turbine is adopted to model the wind generation power output [32].

3.2. SVC Model

The SVC is modelled as a negative generator that can inject or absorb reactive power to provide voltage support. The SVC assumes the role of the capacitive and inductive compensators when it injects or absorbs reactive power, respectively. Electrically, it is shunt connected to buses as shown earlier in Figure 1b. In this paper, the cost function of the SVC is given as the following [33]:

$$C_{SVC,i} = 0.3S_i^2 - 305S_i + 127,380 \ (\$/\text{MVR}), \tag{1}$$

where S_i is the rating or the operating range of the ith SVC. Equation (1) shows that the cost to produce a unit of MVR is higher in the larger SVC and vice versa. In this paper, the ratings of all the SVCs are assumed to be 100 MVR.

3.3. DTR System Model

The IEEE standard 738 relates the rating of bare overhead transmission lines with its environmental conditions such as the following [34]:

$$q_c(\theta, T_a, V_w, \varphi) + q_r(\theta, T_a) = q_s + I^2R(\theta), \tag{2}$$

where the symbol q_c is the convection heat loss. It is calculated as a function of the conductor temperature (θ), ambient temperature (T_a), wind speed (V_w) and the incident wind angle to the conductor (φ). The symbol q_r is the radiated heat loss and it is calculated as a function of the conductor and ambient temperature. The symbol q_s is the heat gain from the solar radiations. $I^2R(\theta)$ is the heat gain from the conductivity of the line, it is also known as the joule heat gain. I is the line current loading in unit Ampere and R is the conductor resistance depending on its temperature. The symbol I can also represents the line current rating if the conductor temperature (θ) is set to maximum. As the conductor temperature capacity depends on the conductor type, a simple ACSR technology is assumed in this paper for all the transmission lines [35]. Under the normal condition without line outages, the conductor temperature is 60 °C, whereas it is 75 °C under the emergency condition that is triggered when line outages occur in the power system.

The functionality of the DTR system depends on the types of sensors, data concentrators and the reliability of the communication system that are used. Although there is no specific literature that describes the cost of the DTR system as a whole, there is a general consensus that it is only a small fraction of the cost needed to install new transmission lines [13,36,37]. In this paper, the investment cost of a new transmission line is assumed to be $350/MW-km and the investment cost of the DTR system is 10% of that value.

3.4. Problem Formulation

The proposed MO planning strategy is presented in this section. The first objective function of the problem formulation is defined as the minimization of the wind curtailment cost such as the following:

$$\min(f_1) = \sum_{t=1}^{T} \lambda_W P_{WC,t}, \tag{3}$$

$$P_{WC,t} = \sum_{i \in \Omega_W} \left(P_{Wi,t}^{\max} - P_{Wi,t}\right), \forall t \in T, \tag{4}$$

where T is the number of simulation hours, λ_W is the wind power curtailment penalty cost that is set to \$50/MWh [8], $P_{WC,t}$ is the wind power curtailment at hour t, $P_{Wi,t}^{\max}$ and $P_{Wi,t}$ are the maximum wind power that is generated and the amount of the connected wind power at the tth hour for the ith wind farm, respectively, and Ω_W is the set of wind farms.

The second objective function consists of the load curtailment cost, fossil fuel cost from the conventional generators, line congestion cost and investment costs from the DTR systems and SVCs. The sum of all these costs is minimized and they are also known as the total social cost such as the following:

$$\min(f_2) = \sum_{i=\Omega_{SVC}} \alpha_i C_{SVC}^{investment} + \sum_{j=\Omega_{DTR}} \beta_j C_{DTR}^{investment} + C_{cong} + C_{LC} + C_{foss}, \tag{5}$$

$$C_{cong} = \sum_{t=1}^{T} \sum_{(i,j) \in \Omega_L} f_{ij,t} \left(\text{LMP}_{j,t} - \text{LMP}_{i,t}\right), \tag{6}$$

$$C_{LC} = \sum_{t=1}^{T} \sum_{i \in \Omega_D} \lambda_D LC_{i,t}, \tag{7}$$

$$C_{foss} = \sum_{t=1}^{T} \sum_{i \in \Omega_G} a_i P_{Gi,t}^2 + b_i P_{Gi,t} + c_i. \tag{8}$$

From Equation (5), the following variables are defined: α_i and β_j are the binary decision variable of the ith SVC unit and the jth DTR system, respectively; Ω_{SVC} and Ω_{DTR} are the set of installed SVCs and DTR systems, respectively; C_{cong} is the line congestion cost; C_{LC} is the load curtailment cost; C_{foss} is the fossil fuel cost of the thermal generator unit. In Equation (6), the variable $f_{ij,t}$ is the power flow in between bus i and j at the tth hour; LMP is the Lagrange multiplier or shadow price of the alternating current optimal power flow (ACOPF); Ω_L is the set of transmission lines. In Equation (7), λ_D is the penalty cost of the load curtailment set as \$2000/MWh [8]; $LC_{i,t}$ is the load curtailment of the ith load point at the tth hour; Ω_D is set of load buses. The load curtailment cost is determined by considering the N-1 criterion in the power network. In Equation (8), a_i, b_i and c_i are the cost coefficients of the ith generator; $P_{Gi,t}$ is the power generated by the ith generator at the tth hour; Ω_G is set of generators.

At each execution of the ACOPF, the following optimization is solved in order to obtain the output levels of the generator units, the LMP values of the network buses and the output responses of the SVCs.

$$\min\left(\sum_{i \in \Omega_G} a_i P_{Gi,t}^2 + b_i P_{Gi,t} + c_i\right), \forall t \in T. \tag{9}$$

This is subject to:

$$\sum_{i \in \Omega_G} P_{Gi,t} + \sum_{i \in \Omega_w} P_{Wi,t} = \sum_{i \in \Omega_D} P_{Di,t}, \forall t \in T, \tag{10}$$

$$\sum_{i \in \Omega_G} Q_{Gi,t} + \sum_{i \in \Omega_{svc}} Q_{SVCi,t} = \sum_{i \in \Omega_D} Q_{Di,t}, \forall t \in T, \tag{11}$$

$$P_{Gi}^{\min} \leq P_{Gi,t} \leq P_{Gi}^{\max}, \forall t \in T, \tag{12}$$

$$Q_{Gi}^{\min} \leq Q_{Gi,t} \leq Q_{Gi}^{\max}, \forall t \in T, \tag{13}$$

$$0 \leq P_{Wi,t} \leq P_{Wi,t}^{\max}, \forall t \in T, \tag{14}$$

$$Q_{SVCi}^{\min} \leq Q_{SVCi,t} \leq Q_{SVCi}^{\max}, \forall t \in T, \tag{15}$$

$$V^{\min} \leq V_i \leq V^{\max}, \forall t \in T, \tag{16}$$

$$\sum_{i=1}^{n} GSF_{l,i} \times (P_{Gi,t} - P_{Di,t}) \leq f_l^{DTR}, \forall t \in T, \tag{17}$$

where $P_{Di,t}$ and $Q_{Di,t}$ are the real and reactive power demand of the *i*th load point at the *t*th hour; $Q_{Gi,t}$ and $Q_{SVCi,t}$ are the reactive power output of the *i*th thermal generators and SVC at the *t*th hour; $Q_{SVCi}^{\min}$ and $Q_{SVCi}^{\max}$ are the minimum and maximum reactive power output of the *i*th SVC; $P_{Gi}^{\min}$ and $P_{Gi}^{\max}$ are the minimum and maximum real power output of the *i*th generator; $Q_{Gi}^{\min}$ and $Q_{Gi}^{\max}$ are the minimum and maximum reactive power output of the *i*th generator; V_i is the voltage level of the *i*th bus; $V^{\min}$ and $V^{\max}$ are the minimum and maximum voltage level of the network bus; $GSF_{l,i}$ is the generation shift factor of line *l* to generator *i*; f_l^{DTR} is the rating of *l*th line after the enhancement by the DTR system. In this ACOPF, the real and reactive load generation balance is given by Equations (10) and (11), respectively. Equations (12) and (13) are the real and reactive power limits of the thermal generator. Equation (14) is the power limits of the wind farm. Equation (15) is the reactive power limits of the SVC. Equation (16) provides the voltage constraints of the network buses. Equation (17) presents the power flow constraints on the transmission lines, in which the line rating is enhanced with the DTR system.

The third objective function consists of minimizing the operation cost of the installed SVCs. This cost is determined by multiplying the average reactive power output of the SVC with the cost of generating one unit of MVR such as the following:

$$\min(f_3) = \sum_{i \in \Omega_{SVC}} EQ_{SVC,i} \times C_{SVC,i}, \tag{18}$$

where $EQ_{SVC,i}$ is the average reactive power output of the *i*th SVC. The value of $C_{SVC,i}$ is from Equation (1).

3.5. Multi-Objective Optimization Method

In the proposed planning strategies as given earlier in Section 2, three different objectives are identified in the optimization procedure. In order to consider all the three conflicting objective functions, a framework such as the MO optimization approach presents an appropriate way to deal with this problem. The reason is it is able to handle both the minimization and maximization of all the objective functions at once, which may have conflicting, supporting or unrelated constraints that affect one another. Due to the characteristic of the constraints, it is normally impossible to optimize all the objective functions at once. As a result, the MO optimization approach normally finds a set of non-dominated optimal solutions, also known as the Pareto optimal solutions [38]. A solution candidate qualifies as the Pareto optimal solution when no objective functions can be improved without degrading the quality of other objective functions. The set of all Pareto optimal solutions is known as the Pareto front. To date, several methods have been proposed to solve the optimization of MO problems [38]. The MO optimization problem presented in this paper has a non-convex and mixed-integer characteristic. For this reason, the genetic-based non-dominated sorting genetic algorithm (NSGA) II are applicable and appropriate [39]. The NSGA II works by sorting a population of solutions into the Pareto front, which are then further ranked according to their non-dominancy level.

3.6. Final Decision Making Method

As described earlier in the MO optimization approach, the solution candidates in the Pareto front are all non-dominant. In other words, they are all equally optimum and applicable as the solutions of the MO optimization problem. Hence, a decision making strategy that can mimic human preferences is needed to select the final solution. The fuzzy method is one such strategy that is appropriate as it can represents decision maker criteria as mathematical equations [40]. The fuzzy method works by assigning a monotonically decreasing set of membership function to each objective and it ranks the Pareto solutions according to the decision maker's criteria about the objective. With this, the degree at which a solution meets the decision maker's preferences is shown. Generally, a zero membership function value denotes total incompatibility, whereas a value of one denotes absolute compatibility. For the minimization problem as described in this paper, a zero and one membership function value is given to the maximum and minimum point of the objective function, respectively. Considering this, the membership function used in this paper is as the following:

$$\mu_{f_i}(X) = \begin{cases} 0, & f_i(X) > f_i^{\max} \\ \frac{f_i^{\max} - f_i(X)}{f_i^{\max} - f_i^{\min}}, & f_i^{\min} \le f_i(X) \le f_i^{\max}, \\ 1, & f_i(X) < f_i^{\min} \end{cases} \tag{19}$$

where $\mu_{f_i}(X)$ is the membership function value for the solution X of the objective function f_i. $f_i^{\min}$ and $f_i^{\max}$ are the minimum and maximum point of the objective function, respectively. After determining the membership function value for each solution on the Pareto front, the final solution is obtained based on the decision maker's preference (μ_i) that is assigned to each objective function, such as the following:

$$\min_{X \in \text{Solution set}} = \sum_{i \in \Omega_f} \left| \mu_i - \mu_{f_i}(X) \right|^n, 1 \le n < \infty, \tag{20}$$

where Ω_f is the set of objective functions. Equation (20) finds the smallest deviation of the membership function values from the decision maker's preference and take that set of solutions as the final decision. The infinity symbol in the equation denotes that the setting of n can be of any large number. However, selecting a larger value will reduce the sensitivity of the final solution towards the preference value.

3.7. Algorithm of the Proposed Approach

The flowchart of the proposed MO optimization algorithm for the placement of the DTR systems and SVCs are shown in Figure 2. The figure shows that the process begins with the initialization of solution population and the loading of the network parameters and weather data. All the network parameters including the customer load data from the IEEE-RTS are used. This information is input into the ACOPF for determining the wind farm generation output, line congestion, amount of load supplied, thermal generation output and responses of SVCs. The ACOPF is repeated according to Equations (9)–(17) until the simulation is converged. Convergence is defined as when the coefficient of variation of the expected-energy-not-supplied (EENS) index is less than or equal to five percent. The EENS is used as a benchmark as it has the longest convergence time among all the other indices [41]. The studies were perform on the second day of 51st week (winter) as this day represent the highest load level throughout the entire year in the IEEE-RTS.

Then, the costs of the three objective functions in Equations (3), (5) and (18) are calculated. Through the concept of the non-dominancy, the first population solution is sorted into the Pareto front. The candidates (children) for the next generation is produced according to the classical genetic algorithm operators such mutation, crossover and elitism. The flow of the proposed algorithm stops when the function tolerance is exceeded. In this paper, this tolerance is defined as the average relative change in the best fitness function value over 100 generations that is less than or equal to 10^{-4}. If the function tolerance is not met, the next solution generations are produced through the selection and recombination process. The new generation of solutions will go through the entire same procedure starting again from the ACOPF stage as shown in Figure 2. When the function tolerance is exceeded, a set of non-dominated solutions (Pareto front) is considered obtained. The fuzzy decision making method is applied onto the Pareto front to obtain the final optimal solution.

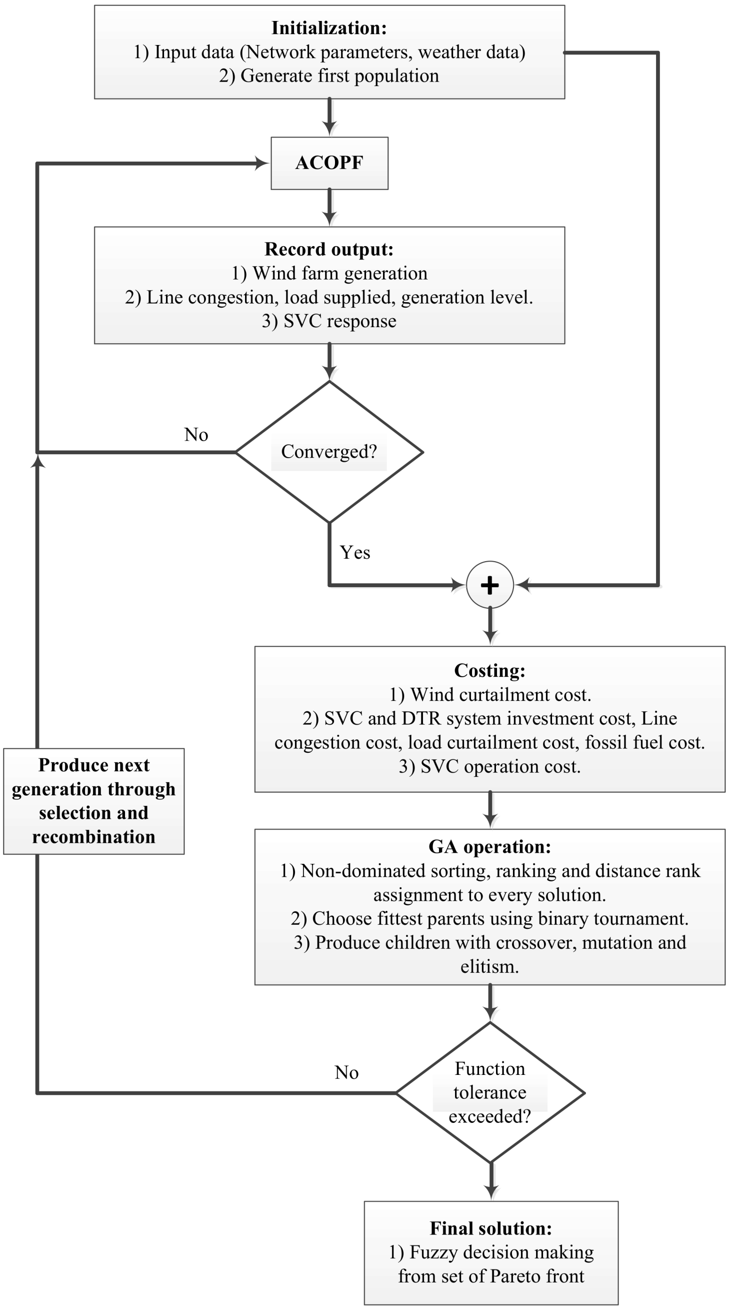

Figure 2. Flowchart of the proposed algorithm. ACOPF: alternating current optimal power flow; DTR: dynamic thermal rating.

3.8. Test System

The proposed algorithm was implemented in MATLAB and the ACOPF was performed using an open source software, MATPOWER [42]. The IEEE-RTS was used as the test system [30]. The original RTS was modified by raising the load and the generation levels by twofold, making the new peak load and generation as 5700 MW and 6810 MW, respectively. The original ratio of the reactive and real powers is maintained in the modified network. The purpose of this increment is to simulate a future situation whereby electricity users grow substantially. Moreover, 3000 MW of wind energy, divided equally among three wind farms was also added into the original RTS. They are located at bus 4, 14 and 17 as shown in the single-line diagram of the modified IEEE-RTS in Figure 3.

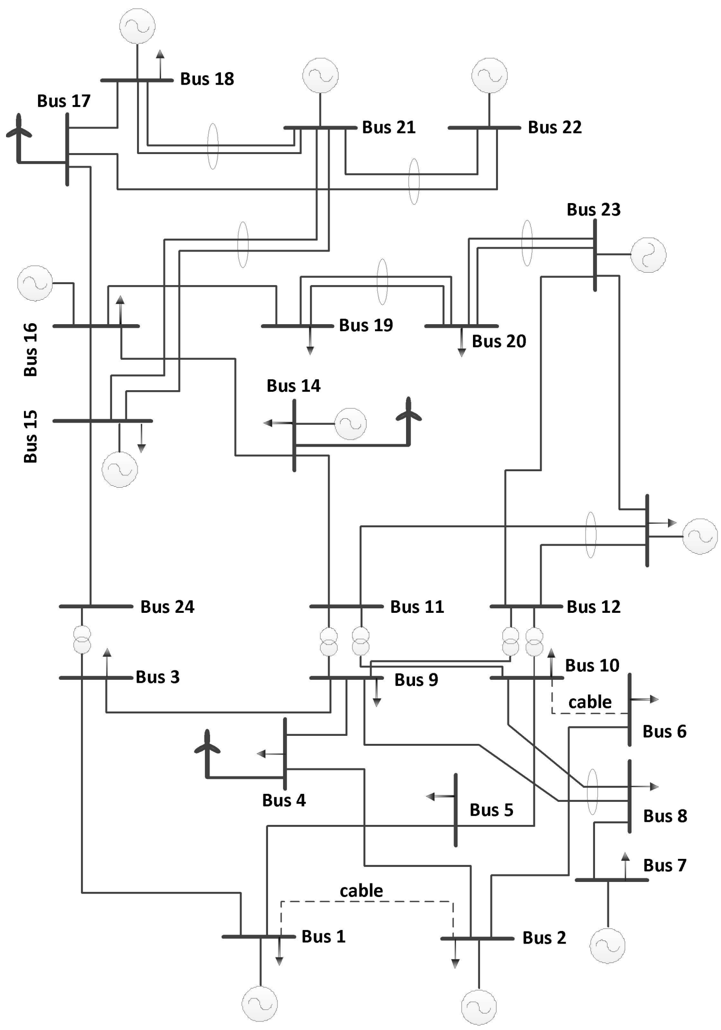

Figure 3. Modified IEEE reliability test system (IEEE-RTS).

Since the SVC and DTR systems are used to enhance the network for maximizing the integration of wind energy, 10 candidate buses and transmission line corridors that are most sensitive towards the reduction of wind curtailment after the enhancement are identified. The remaining not shortlisted buses and lines are not considered for the placement of the SVCs and DTR systems in the proposed algorithm. For the candidate buses, the sensitivity of wind curtailment subject to the voltage and reactive power limitations of bus b is defined as the marginal decrease in the total wind curtailment due to the reactive power support increment of the corresponding bus such as [43]:

$$s_b = \frac{\partial P_{WC}}{\partial Q_b}, \tag{21}$$

where s_b is the sensitivity of bus b as described earlier, δP_{WC} is the marginal reduction of wind energy curtailment and δQ_b is the marginal increment of reactive power injection at bus b. As for the candidate line, the sensitivity of wind curtailment subject to the congestion of line l is defined as the marginal decrease in the total wind curtailment due to capacity increment of the corresponding line such as:

$$s_l = \frac{\partial P_{WC}}{\partial f_l}, \tag{22}$$

where s_l is the sensitivity of line l and δf_l is the marginal capacity increment of line l.

In order to determine the s_b for every bus, a reactive power source of 1 MVR was injected into each bus one at a time while maintaining all other parameters. The buses were then ranked according to their ability to reduce the wind energy curtailment. The top 10 best buses as according to Equation (21) were selected and they are bus 3, 4, 6, 8, 9, 10, 11, 15, 16 and 24. In a similar effort, the s_l for every line were determined by raising the capacity of the line by one-megawatt one at a time while maintaining all other parameters. The lines were also ranked according to their ability to reduce the wind energy curtailment. The top 10 best lines as according to Equation (22) were selected and they are lines between bus 3-24, 5-10, 8-9, 1-3, 3-9, 2-4, 15-16, 17-18, 7-8 and 4-9.

From the above descriptions, wind speed and the DTR systems weather data from three and ten locations, respectively, are needed. The wind speed data is used to model the wind farm power output and the DTR systems weather data is used to calculate the hourly line rating of the transmission corridors. All the required weather data was sampled from the British Atmospheric Data Centre (BADC) website [44].

4. Results and Discussion

The proposed algorithm was executed by considering the three objective functions mentioned in Section 3. The NSGA II algorithm was implemented in MATLAB using the default population size of 200. The non-dominated solutions are shown in Figure 4, whereby the objective function equivalent daily values are presented. The figure shows that the optimal wind curtailment cost vary from 0.7 to 1.1 M$, the optimal total social cost vary from 3 to 9 M$, and the optimal SVC operation cost vary from 0.1 to 10 M$.

The results in Figure 4a shows that as the investment for the total social cost decreases, the amount of wind energy curtailment increases and vice versa. The reason is the lack of the SVCs and DTR systems inhibit the capability of the power system to absorb more wind energy. The rate at which the wind curtailment cost decreases with the increment of the total social cost, however, depends on the complex power system policies and regulations as well as the wind energy penalty cost. It is noticed that although more wind energy utilization leads to the lower usage of conventional thermal generators and hence the fossil fuel cost, the total social cost continue to increase. This is due to the offset of the fossil fuel cost saving by the extra investment needed for the installation and operation of the SVCs and DTR systems.

Another observation from Figure 4a is that certain portions of the Pareto front indicate fast increment in the total social cost, especially when wind curtailment cost is 0.8 M$ and below. These increments represent the additional SVC units that impose relatively high investment cost as compared to the DTR systems. Considering this, the portions of the Pareto front that have slow total social cost increment represent the solutions which has suggested the installation of more DTR systems than the SVC. From Figure 4b, as the wind energy curtailment cost is reduced, the SVC operation cost is increased. The reason is more reactive power support is needed by the power network in order to absorb wind energy while maintaining voltage limits of the network. In Figure 4c, as the total social cost increases by adding more SVC, the operation cost of the SVC also increases in order to maximize wind energy connection. The empty portion of the graph is due to the addition of the DTR systems are instead of the SVC. The relatively much lower cost of the DTR system as compared to the SVC causes only marginal increase in the total social cost and, hence, a huge leap in the value of the total social cost when the SVCs are added at around the seven million dollar mark.

One of the advantages of the multi-objective optimization method is that the decision makers can determine the desired levels (μ_i) for each objective function in order to choose the final optimal solutions from the Pareto front. Normally, these levels are influenced by the renewable energy policies adopted by the decision makers. Due to this feature, the selected values of μ_i will reflect the importance of each objective function. From the results in Figure 4, the final optimal solutions were selected using the fuzzy final decision making method as presented in Section 3.6. These results, with three sets of decision maker's preference values, are presented in Table 1. The presented results in Table 1 show the optimal buses and lines for locating the SVC and DTR system as well as all the objective function values.

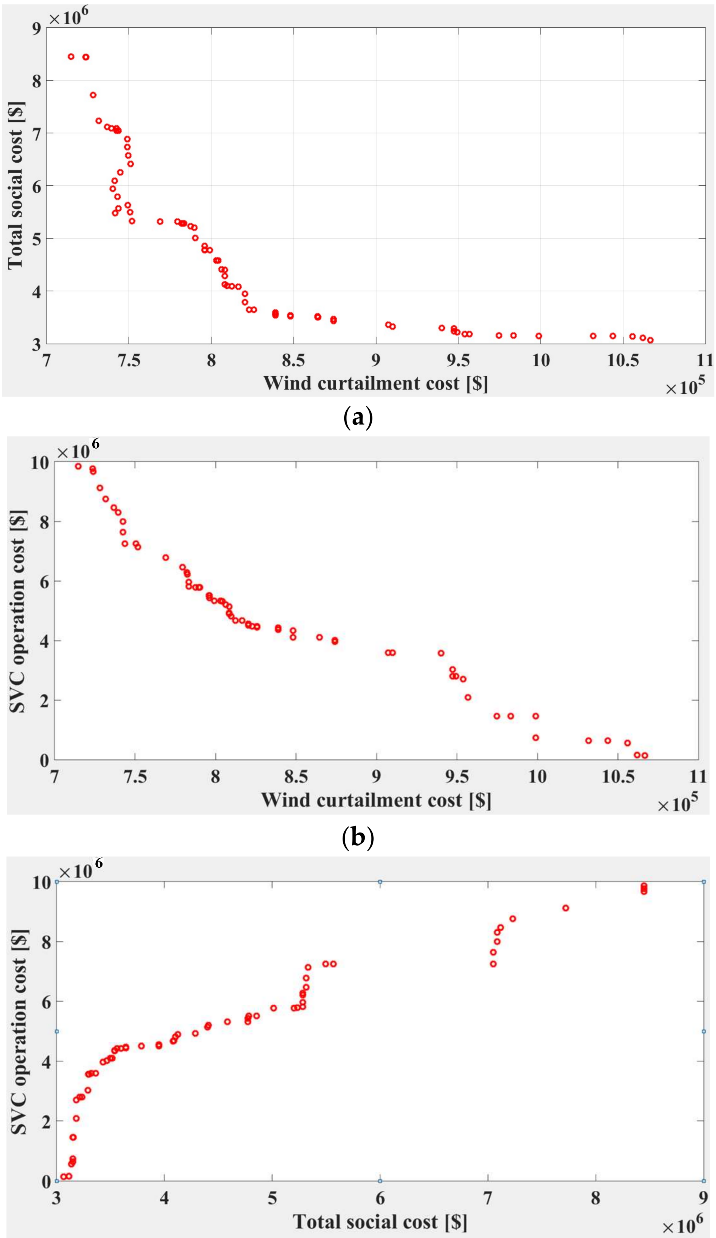

Figure 4. Various non-dominated solutions: (**a**) Total social cost vs. wind curtailment cost. (**b**) SVC operation cost vs. wind curtailment cost. (**c**) SVC operation cost vs. total social cost.

Table 1. Final optimal solutions of different membership function values.

		μ_1 = 0.8, μ_2 = 0.5, μ_3 = 0.5	μ_1 = 1, μ_2 = 0.5, μ_3 = 0.5	μ_1 = 1, μ_2 = 0.5, μ_3 = 0.8
Placement	Optimal bus for SVC	6, 15, 16, 24	3, 6, 9, 11	3, 6, 9, 11, 15
	Optimal line for DTR system	4-18, 8-16, 9-17, 9-23, 11-21, 19-37	1-26, 2-14, 4-18, 8-16, 9-23, 11-21, 19-37	4-18, 6-15, 8-16, 9-17, 19-37
Cost	Wind curtailment cost (M$)	0.8063	0.7962	0.8258
	Total social cost (M$)	4.4088	4.7846	3.6439
	SVC operation cost (M$)	5.1953	5.5119	4.4377

In the first set of the solutions, more emphasis is given towards the minimization of wind energy curtailment, whereas the total social and SVC operation costs have equal importance. In the second set, the membership function value of wind energy curtailment is increased to 1. Under this selection criteria, the wind energy curtailment cost is reduced while the total social and SVC operation costs are increased to achieve this goal. As a result, more DTR systems are installed in this set as well. The final set of the solutions allocate additional preference towards the minimization of the SVC operation cost. Under this selection criteria, the SVC operation cost decreases while the wind energy curtailment and total social costs increase slightly.

Sensitivity Analysis

The results obtained through the multi-optimization problem formulation as shown in Figure 4 are influenced by the various penalty values used in the proposed algorithm; different penalty values will impact the final optimal decisions. In order to investigate these impacts, sensitivity analyses were carried out. Figure 5 shows the impacts of various enhancement strategies toward the level of wind energy curtailment throughout the day. The result indicating the "Optimal plan" is the enhancement configuration of the first solution set from Table 1. Other options such as the "DTR system only" and "SVC only" have the same configuration settings as the "Optimal plan", but with the application of either the DTR system or SVC only, respectively. The "Nothing" option means that neither the DTR system nor SVC was used to enhance the power network. The results from Figure 5 show that the "Optimal plan" is able to keep the wind curtailment level at its lowest and this is followed by the "DTR system only", "SVC only" and the "Nothing" plan. The "DTR system only" plan performs better than the "SVC only" plan shows that the former has a larger impact towards the reliability of the power network. The reason is the DTR system is able to enhance line ratings for most of the time depending mainly on the weather conditions and it is not affected by network parameters. On the other hand, the "SVC only" plan is affected by AC transmission network parameters and has lesser reliability influence due to the minimum power generation constrain that is needed to maintain power system dynamic stability. Hence, the SVC can only contribute to the reduction of wind curtailment when existing reactive power compensations supply by the generators are inadequate. Besides that, the injection of reactive power support from the SVC is also sometimes limited by bus terminal voltage requirements. Considering all these, the full potential of the SVC might sometimes not able to be realized, leading to more wind curtailment than the "DTR system only" plan.

In Figure 6, the investment cost of the DTR system is varied, whereby the original DTR system cost that was taken as 10% of the cost of building a new line is modified to 20% and 5%. The effects of these costs towards the "Optimal plan" are shown in the figure. The results show that as the DTR system cost increases, the amount of wind curtailment increases as well. This observation make sense as the DTR system becomes more expensive, less of it will be installed in order to lower the total social cost while allowing a higher wind curtailment. On the contrary, when the DTR system becomes cheaper, the wind curtailment level is reduced. The reason for this is as the DTR system cost is reduced, more of it can be afforded leading to the overall reduction of wind curtailment without excessively increasing the total social cost. Regardless of the considered options, the differences among the results are not huge due to both the total social and wind curtailment costs that always reach non-dominancy forming the Pareto front as a result of the NSGA II employed in the proposed algorithm. Moreover, the impact of the DTR system towards the total social cost is also not significant due to the relatively much higher cost of the SVC device.

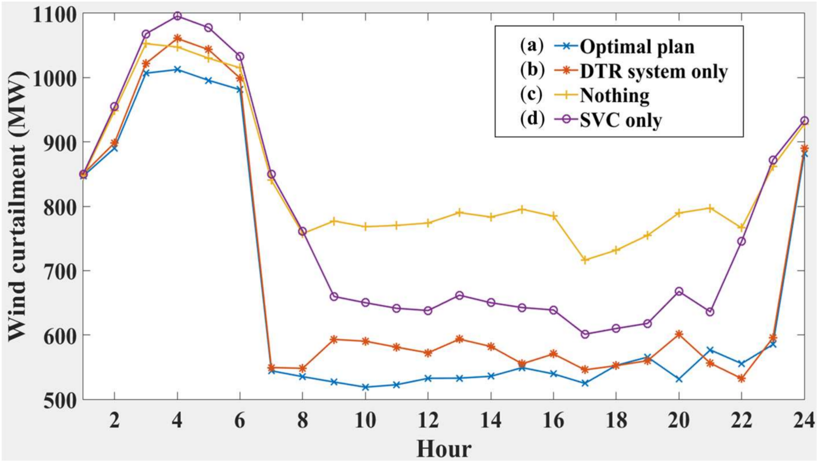

Figure 5. Wind energy curtailment level using the (**a**) optimal plan, (**b**) optimal plan but with the DTR system only (DTR system only), (**c**) optimal plan but with the SVC only (SVC only), and (**d**) without any enhancement (Nothing).

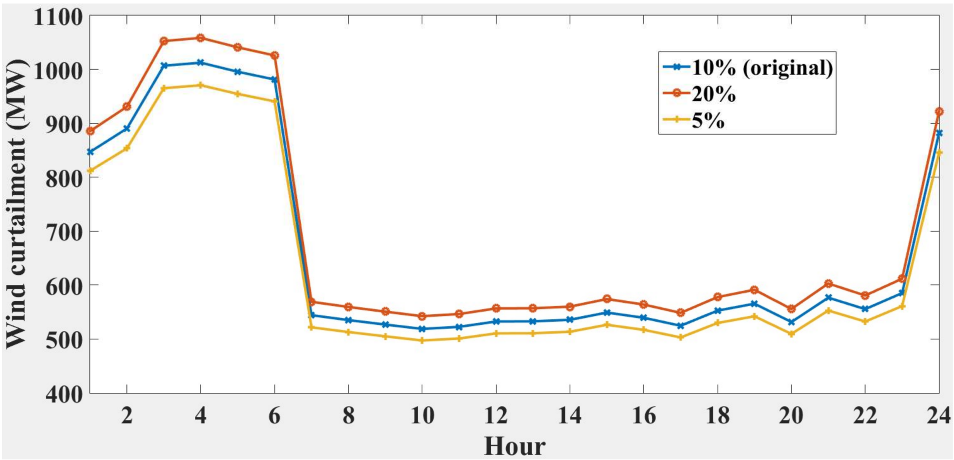

Figure 6. Wind energy curtailment level at various DTR system investment costs.

5. Conclusions

This paper proposes a power network planning algorithm that considers various objective functions separately. These objectives are the minimization of wind curtailment, total social cost and SVC operation cost. Due to the nature of the multi-objective posterior framework algorithm, the Pareto front that contains all the optimal solutions were found using the NSGA II. Among the Pareto front, a final optimal solution was determined using the fuzzy decision making method that can emulate decision maker's preferences. The proposed method was tested on the IEEE-RTS and the robustness of the proposed algorithm was demonstrated. It was shown that the algorithm of this paper can aid power system operators in managing wind energy integration issues in order to avoid penalty cost. The DTR system is effective in raising the transmission line capacity and the SVC is useful in providing reactive power support for improving the loadability of the line. Hence, the DTR system and the SVC are good complements for each other.

Acknowledgments: This work is partly supported by the USM Short Term grant: 304.PELECT.60313051 and the USM Bridging grant: 304.PELECT.6316117 and the Ministry of Science and Technology (MOST) in Taiwan under grants MOST 105-2221-E-027-096, MOST 105-2221-E-324-02, MOST 105-2221-E-324-026, and MOST 106-2218-E-027-010.

Author Contributions: Jiashen Teh and Ching-Ming Lai conceived and designed the experiments; Yu-Huei Cheng contributed reagents/materials/analysis tools; Jiashen Teh wrote the paper.

Conflicts of Interest: The authors declare no conflict of interest.

References

1. Global Wind Energy Council (GWEC). *Global Wind Report 2016—Annual Market Update*; Global Wind Energy Council: Brussels, Belgium, 2016.
2. European Comission. *Energy Roadmap 2050 [COM/2011/885]*; European Comission: Brussels, Belgium, 2011.
3. Haileselassie, T.M.; Uhlen, K. Power System Security in a Meshed North Sea HVDC Grid. *Proc. IEEE* **2013**, *101*, 978–990. [CrossRef]
4. Burke, D.J.; Malley, M.J.O. Factors Influencing Wind Energy Curtailment. *IEEE Trans. Sustain. Energy* **2011**, *2*, 185–193. [CrossRef]
5. RTE. *Business and Sustainable Development Report*; RTE: Paris, France, 2015.
6. Gautam, D.; Vittal, V.; Harbour, T. Impact of Increased Penetration of DFIG-Based Wind Turbine Generators on Transient and Small Signal Stability of Power Systems. *IEEE Trans. Power Syst.* **2009**, *24*, 1426–1434. [CrossRef]
7. Billinton, R.; Wangdee, W. Reliability-Based Transmission Reinforcement Planning Associated with Large-Scale Wind Farms. *IEEE Trans. Power Syst.* **2007**, *22*, 34–41. [CrossRef]
8. Park, H.; Baldick, R. Transmission Planning Under Uncertainties of Wind and Load: Sequential Approximation Approach. *IEEE Trans. Power Syst.* **2013**, *28*, 2395–2402. [CrossRef]
9. Moeini-Aghtaie, M.; Abbaspour, A.; Fotuhi-Firuzabad, M. Incorporating Large-Scale Distant Wind Farms in Probabilistic Transmission Expansion Planning—Part I: Theory and Algorithm. *IEEE Trans. Power Syst.* **2012**, *27*, 1585–1593. [CrossRef]
10. Moeini-Aghtaie, M.; Abbaspour, A.; Fotuhi-Firuzabad, M. Incorporating Large-Scale Distant Wind Farms in Probabilistic Transmission Expansion Planning—Part II: Case Studies. *IEEE Trans. Power Syst.* **2012**, *27*, 1594–1601. [CrossRef]
11. Orfanos, G.A.; Georgilakis, P.S.; Hatziargyriou, N.D. Transmission Expansion Planning of Systems with Increasing Wind Power Integration. *IEEE Trans. Power Syst.* **2013**, *28*, 1355–1362. [CrossRef]
12. Fernandes, C.; Frías, P.; Olmos, L. Expanding interconnection capacity to integrate intermittent generation in the Iberian Peninsula. *IET Renew. Power Gener.* **2013**, *7*, 45–54. [CrossRef]
13. WG B2.13. Guidlines for Increased Utilization of Existing Overhead Transmission Line. In *CIGRE Brochure*; 2008; Available online: https://e-cigre.org/publication/353-guidelines-for-increased-utilization-of-existing-overhead-transmission-lines (accessed on 26 March 2018).
14. Matevosyan, J. Wind Power Integration in Power Systems with Transmission Bottlenecks. In Proceedings of the 2007 IEEE Power Engineering Society General Meeting, Tampa, FL, USA, 24–28 June 2007; pp. 1–7.
15. Teh, J.; Cotton, I. Critical span identification model for dynamic thermal rating system placement. *IET Gener. Transm. Distrib.* **2015**, *9*, 2644–2652. [CrossRef]
16. Teh, J.; Cotton, I. Reliability Impact of Dynamic Thermal Rating System in Wind Power Integrated Network. *IEEE Trans. Reliab.* **2016**, *65*, 1081–1089. [CrossRef]
17. Greenwood, D.M.; Ingram, G.L.; Taylor, P.C. Applying Wind Simulations for Planning and Operation of Real-Time Thermal Ratings. *IEEE Trans. Smart Grid* **2017**, *8*, 537–547. [CrossRef]
18. Ali, M.; Degefa, M.Z.; Humayun, M.; Safdarian, A.; Lehtonen, M. Increased Utilization of Wind Generation by Coordinating the Demand Response and Real-time Thermal Rating. *IEEE Trans. Power Syst.* **2016**, *31*, 3737–3746. [CrossRef]
19. Ara, A.L.; Kazemi, A.; Niaki, S.A.N. Multiobjective Optimal Location of FACTS Shunt-Series Controllers for Power System Operation Planning. *IEEE Trans. Power Deliv.* **2012**, *27*, 481–490. [CrossRef]
20. Zhu, J.; Cheung, K.; Hwang, D.; Sadjadpour, A. Operation Strategy for Improving Voltage Profile and Reducing System Loss. *IEEE Trans. Power Deliv.* **2010**, *25*, 390–397. [CrossRef]

21. Ghahremani, E.; Kamwa, I. Optimal placement of multiple-type FACTS devices to maximize power system loadability using a generic graphical user interface. *IEEE Trans. Power Syst.* **2013**, *28*, 764–778. [CrossRef]
22. Hossain, M.J.; Pota, H.R.; Mahmud, M.A.; Ramos, R.A. Investigation of the Impacts of Large-Scale Wind Power Penetration on the Angle and Voltage Stability of Power Systems. *IEEE Syst. J.* **2012**, *6*, 76–84. [CrossRef]
23. Alhasawi, F.B.; Milanovic, J.V. Techno-Economic Contribution of FACTS Devices to the Operation of Power Systems with High Level of Wind Power Integration. *IEEE Trans. Power Syst.* **2012**, *27*, 1414–1421. [CrossRef]
24. Nasri, A.; Conejo, A.J.; Kazempour, S.J.; Ghandhari, M. Minimizing Wind Power Spillage Using an OPF With FACTS Devices. *IEEE Trans. Power Syst.* **2014**, *29*, 2150–2159. [CrossRef]
25. Billinton, R.; Karki, R. Maintaining supply reliability of small isolated power systems using renewable energy. *IEE Proc. Gener. Transm. Distrib.* **2001**, *148*, 530–534. [CrossRef]
26. Bouffard, F.; Galiana, F.D. Stochastic Security for Operations Planning with Significant Wind Power Generation. *IEEE Trans. Power Syst.* **2008**, *23*, 306–316. [CrossRef]
27. Burke, D.J.; Malley, M.J.O. Maximizing Firm Wind Connection to Security Constrained Transmission Networks. *IEEE Trans. Power Syst.* **2010**, *25*, 749–759. [CrossRef]
28. Salehi-Dobakhshari, A.; Fotuhi-Firuzabad, M. Integration of large-scale wind farm projects including system reliability analysis. *IET Renew. Power Gener.* **2011**, *5*, 89–98. [CrossRef]
29. Abdullah, M.A.; Muttaqi, K.M.; Sutanto, D.; Agalgaonkar, A.P. An Effective Power Dispatch Control Strategy to Improve Generation Schedulability and Supply Reliability of a Wind Farm Using a Battery Energy Storage System. *IEEE Trans. Sustain. Energy* **2015**, *6*, 1093–1102. [CrossRef]
30. Subcommittee, P.M. IEEE Reliability Test System. *IEEE Trans. Power Appar. Syst.* **1979**, *PAS-98*, 2047–2054. [CrossRef]
31. Billinton, R.; Chen, H.; Ghajar, R. Time-series models for reliability evaluation of power systems including wind energy. *Microelectron. Reliab.* **1996**, *36*, 1253–1261. [CrossRef]
32. Vestas. Available online: https://www.vestas.com/en/products/turbines (accessed on 26 March 2018).
33. Cai, L.J.; Erlich, I.; Stamtsis, G. Optimal Choice and Allocation of FACTS Devices in Deregulated Electricity Market Using Genetic Algorithms. In Proceedings of the IEEE PES Power Systems Conference and Exposition, New York, NY, USA, 10–13 October 2004; Volume 1, pp. 201–207.
34. IEEE. *IEEE Standard for Calculating the Current-Temperature of Bare Overhead Conductors*; IEEE Std 738-2006 (Revision of IEEE Std 738-1993); IEEE: Piscataway Township, NJ, USA, 2007. [CrossRef]
35. Kopsidas, K.; Kapetanaki, A.; Levi, V. Optimal Demand Response Scheduling with Real Time Thermal Ratings of Overhead Lines for Improved Network Reliability. *IEEE Trans. Smart Grid* **2017**, *8*, 2813–2825. [CrossRef]
36. WG B2.06. How Overhead Lines Are Redesignd for Uprating/upgrading-Analysies of the Replies to the Questionnaire. In *Cigre Brochure*; 2006; Available online: https://e-cigre.org/publication/294-how-overhead-lines-are-redesignd-for-upratingupgrading-analysies-of-the-replies-to-the-questionnaire (accessed on 26 March 2018).
37. CIGRE. *Increasing Capacity of Overhead Transmission Lines: Needs and Solutions*; Technical Brochure; CIGRE: Paris, France, 2010.
38. Varadarajan, M.; Swarup, K.S. Solving multi-objective optimal power flow using differential evolution. *IET Gener. Transm. Distrib.* **2008**, *2*, 720–730. [CrossRef]
39. Srinivas, N.; Deb, K. Muiltiobjective Optimization Using Nondominated Sorting in Genetic Algorithms. *Evolut. Comput.* **1994**, *2*, 221–248. [CrossRef]
40. Deb, K. *Multi-Objective Optimization Using Evolutionary Algorithm*; Wiley: Chichester, UK, 2001; Volume 2012.
41. Billinton, R.; Allan, R.N. *Reliability Evaluation of Power Systems*; Plenum: New York, NY, USA, 1984.
42. Zimmerman, R.D.; Murillo-Sanchez, C.E. *MATPOWER 5.0 User's Manual*; Power System Engineering Research Center (PSERC), Arizona State University: Tempe, AZ, USA, 2014.
43. Gu, Y.; Xie, L. Fast Sensitivity Analysis Approach to Assessing Congestion Induced Wind Curtailment. *IEEE Trans. Power Syst.* **2014**, *29*, 101–110. [CrossRef]
44. British Atmospheric Data Center (BADC). Available online: http://badc.nerc.ac.uk/home/ (accessed on 26 March 2018).